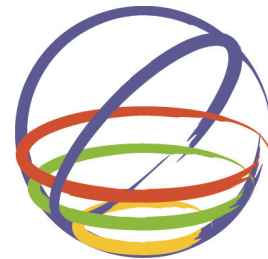


Numerical Study of Three-Dimensional Nonlinear Behavior of Soil-Pile-Structure System under Strong Input Motion



Youhao Zhou, Kohji Tokimatsu & Hiroko Suzuki

Tokyo Institute of Technology, Japan

Hiroyuki Yoshida

Tokyo Electric Power Service Co., Ltd., Japan

Yasushi Nukui

Tokyo Electric Power Company, Japan

15 WCEE
LISBOA 2012

SUMMARY:

Numerical simulation of soil-pile-structure model subjected to strong shaking was performed to examine the factors affecting the three-dimensional nonlinear dynamic behavior of pile foundation while soil shows strong nonlinearity. The tests were conducted using the large-scale shaking table at the E-Defense to investigate the response and failure of a nearly full-scale pile-structure system under multi-dimensional loading. The analysis was unable to predict the yielding of the pile very accurately. However, in general, the analysis was able to reproduce the three-dimensional nonlinear behaviors of the piles with a reasonable degree of accuracy when only a few piles have yielded in the test, suggesting its certain applicability to soil-pile-structure system subjected to strong 3-D shaking.

Keywords: Shaking table test, Pile, Three-dimensional finite element method, Dynamic interaction, Nonlinearity

1. INTRODUCTION

Most of Japanese metropolises lie on soft ground near seas and large rivers. For this reason, pile foundations are commonly applied for substructures. Pile foundations are, however, weak in horizontal direction and tend to be damaged by both inertial force from superstructures and kinematic force from ground displacement during earthquakes. Such pile damage is considered to be the result of three-dimensional nonlinear interaction of soil-pile-structure system (Koyamada et al., 2005; Nakazawa et al., 1999).

Numerous studies, both experimental and numerical, have been carried out to study the soil-pile-structure interaction and nonlinear behavior of piles during earthquakes. However, most experimental studies are limited to one-dimensional shaking, thus the three-dimensional dynamic behavior of soil-pile-structure system is not fully discussed. Furthermore, since the nonlinearization of near-pile soil is considered to progress due to the soil-pile-structure interaction, it is unclear whether the three-dimensional analysis method expanded from one-dimensional analysis can reproduce such nonlinear behavior of soil and piles during earthquakes.

In order to obtain sufficient data to establish a design method for pile foundation with failure of piles taken into account, a series of shaking table tests using soil-pile-structure models were performed (MEXT and NIED, 2006; Suzuki et al., 2010; Tokimatsu et al., 2007). In a previous study, test cases subjected to moderate shaking were studied by performing dynamic nonlinear analysis using three-dimensional finite element method, and the analysis was able to reproduce the test results with a reasonable degree of accuracy (Zhou et al., 2012). This paper focuses on the test case subjected to strong shaking where several piles yielded, and discusses the factors influencing the three-dimensional nonlinear behaviors of pile foundation, by examining the test results and performing numerical analysis.

2. SHAKING TABLE TESTS

The E-Defense shaking table platform has a dimension of 15 m length and 20 m width. Fig. 2.1 and Fig. 2.2 show the test model constructed in a cylindrical laminar shear box 6.5 m high with an inside diameter of 8.0 m. It consists of forty-one stacked ring frames, allowing two-dimensional shear deformation of the inside soil.

A 3x3 steel pile group supporting a footing with or without a superstructure was used for the tests. The piles were labelled A1 to C3 according to their locations within the pile group, as shown in Fig. 2.2. Each pile had a diameter of 152.4 mm and a wall thickness of 2.0 mm. The piles were set up with a horizontal space of four-pile diameters center to center. Their tips were jointed to the laminar box base with pins and their heads were fixed to the footing of a weight of 10 tons.

Dry Albany sand from Australia was used for preparing the sand deposit. Fig. 2.3 shows the grain size distribution of the sand. The sand had a mean grain size D_{50} of 0.31 mm and a coefficient of uniformity U_c of 2.0. After setting a pile group in the laminar box, the dry sand was air-pluviated and compacted at every 0.275m to a relative density of about 70% to form a uniform sand deposit with a thickness of 6.3m.

As listed in Table 2.1, a total of five test series named A to E was conducted in alphabetical order, in

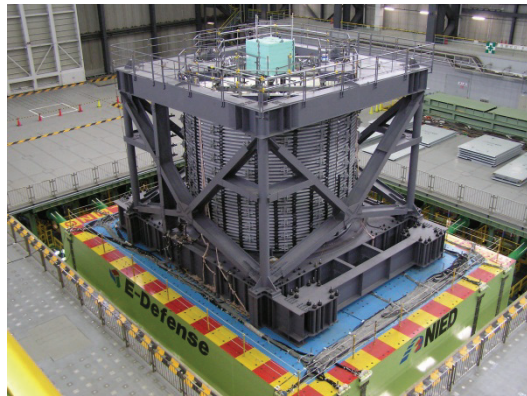


Figure 2.1. Test model on large shaking table

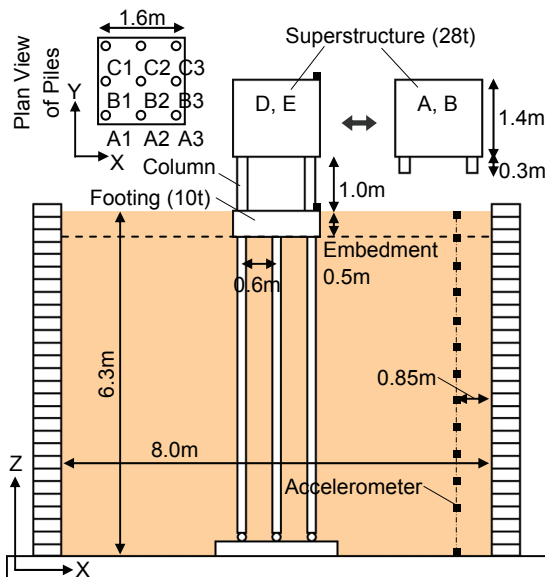


Figure 2.2. Soil-pile-structure model

Table 2.1. Test model series

	Embedment	Superstructure	Natural frequency (Hz)
A	Yes	Yes	10.0
B	Yes	Yes	1.67
C	Yes	No	-
D	Yes	Yes	5.0
E	No	Yes	5.0

Table 2.2. Shaking conditions of test series

	Maximum input acceleration (m/s^2)			
	JR Takatori		Taft, Tottori	
	XYZ	XY,X,Y	XYZ	XY,X,Y
A	0.3, 0.8			
B	0.3, 0.8		0.3, 0.8	-
C	0.3, 0.8			
D	0.3, 0.8		0.3, 0.8	
E	0.3, 0.8 6.0, 8.0	0.3, 0.8	0.3, 0.8 (Taftonly)	-

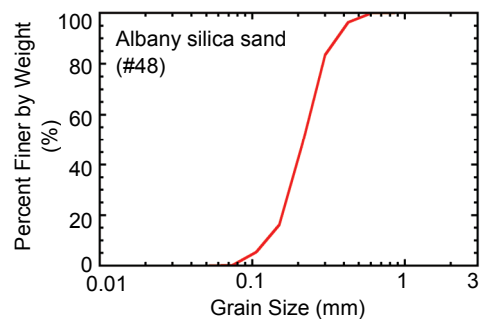


Figure 2.3. Grain size distribution of Albany sand

which the presence of footing embedment and superstructure, and the natural frequency of superstructure, were varied.

Table 2.2 shows the list of shaking conditions of test series. The tests were conducted under one-, two- or three-dimensional shaking with three types of ground motions, which dominate in different frequency ranges, with maximum horizontal accelerations adjusted to 0.3 m/s^2 and 0.8 m/s^2 . In addition, in order to investigate the pile destruction process induced by ground motion, additional tests were conducted for series E, under three-dimensional shaking using JR Takatori wave with maximum horizontal accelerations at 6.0 m/s^2 and 8.0 m/s^2 .

Among the cases conducted with the three-dimensional JR Takatori wave, this paper focuses on the one in test series E, with maximum acceleration adjusted to 6.0 m/s^2 . The soil showed nonlinear behavior and some of the piles yielded during the test.

3. ANALYTICAL MODEL

Dynamic nonlinear analysis was conducted with a three-dimensional finite element model using analysis code EENA3D developed by TEPCO (Yoshida et al., 2006; Yoshida et al., 2008). Fig. 3.1 and 3.2 show the outline of analysis model and the detail of piles and footing, respectively.

The laminar shear box is modelled as solid elements with equivalent mass and adequately small stiffness. The degree of freedom is restrained, so that each ring frame of the shear box can maintain its plane during shear deformation. To take the effect of rocking behavior of the shaking table into account, vertical springs are placed at eight points at the bottom of the box.

The piles are modelled as beam elements. As shown in Fig. 3.3, an axial force dependent bilinear $M-\phi$ relation is used for nonlinear model of the piles. The yield bending moments are calculated according to Recommendations for the Plastic Design of Steel Structures (AIJ, 1975). The reduction of axial stiffness after piles' yielding is not considered. Areas of the piles are set as void, and the piles are connected to the soil with massless rigid beam elements, maintaining pile sections. In order to consider the friction and separation between piles and soil, joint elements are inserted in between. Strengths of the joint elements are set according to the internal friction angle of sand mentioned later. The pile head rigidity was set to 0.86, by performing parametric study with the test cases subjected to smaller input motion.

The columns supporting a superstructure are modelled as beam elements. The rigidity of column tips is adjusted according to the peak period of footing-superstructure transfer function from the test.

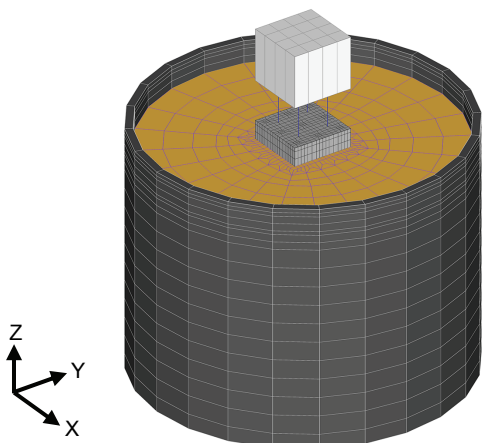


Figure 3.1. Overview of analysis model

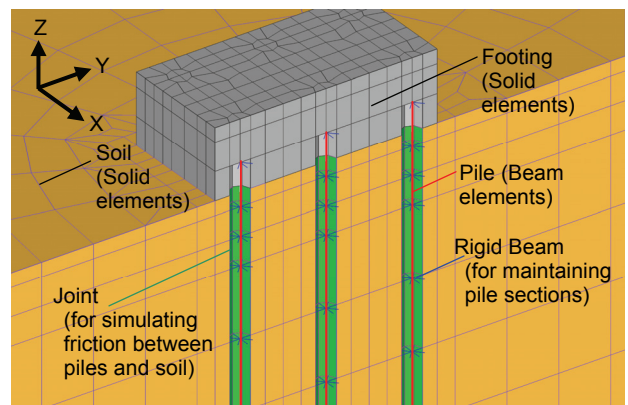


Figure 3.2. Details of piles in analysis model

Table 3 explains specifications of the soil. Velocities of P and S waves, V_P and V_S , are obtained by performing regression analysis on the results of PS logging depending on overburden pressure σ'_v . Poisson's ratio ν is calculated from V_P and V_S . The cohesion c and internal friction angle φ of the soil are obtained from laboratory test.

Fig. 3.4 explains dynamic strain dependency of the soil. In EENA3D, nonlinearity of the soil is simulated by directly inputting the discrete data of $G/G_0-\gamma$ regression curve, referring to Yoshida et al. (1990). $\tau-\gamma$ relation is then calculated also as discrete data, to be linearly interpolated to define skeleton curve. Failure of the soil is defined by the second constant J_2 of deviatoric stress q , based on von Mises' failure criterion. Three-dimensional constitutive rule is, referring to Yoshida et al. (1993), defined by stress-strain relation given by Eqn. 3.1;

$$\sigma_e = G \cdot e \quad (3.1)$$

where σ_e is equivalent stress and e is equivalent strain, which are expressed by root of deviatoric stress q and deviatoric strain ε_s , respectively. Based on Eqn. 3.1, by substituting equivalent stress σ_e for shear stress τ and equivalent strain e for shear strain γ , nonlinearity of the soil is expressed by the dynamic strain dependencies ($G/G_0-\gamma$ and $h-\gamma$). However, since both the equivalent stress σ_e and the equivalent strain e take only positive values, it is impossible to identify whether it is pulsating or alternating, making it impossible to properly draw hysteresis curve. As a countermeasure, the radius of yield surface in π plane is given as increment of deviatoric strain e .

The input motion, as shown in Fig. 3.5, was calculated by averaging each component of eight observed records, four obtained at the bottom of the shear box and four at the bottom of the sand deposit. The input motion was applied to the bottom center of the analysis model to perform three-dimensional nonlinear dynamic analysis.

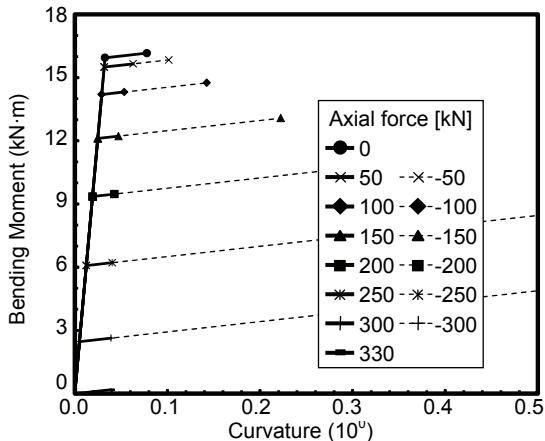


Figure 3.3. Axial force dependent model of piles

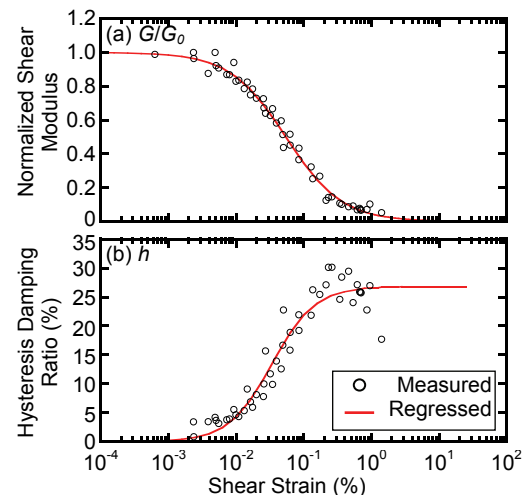


Figure 3.4. Dynamic strain dependency of soil

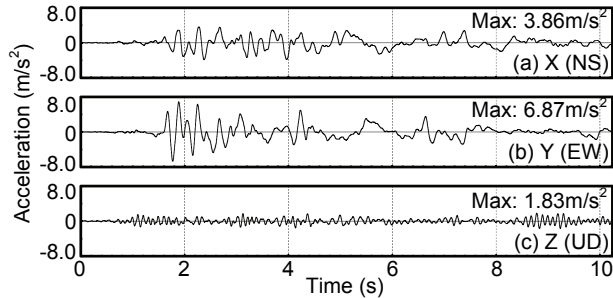


Figure 3.5. Input motion

Table 3.1. Specifications of soil

Parameter	Value
Density ρ (t/m^3)	1.71
S wave velocity V_S (m/s)	$85.9\sigma'_v^{0.25}$
P wave velocity V_P (m/s)	$145.9\sigma'_v^{0.25}$
Poisson's ratio ν	0.23
Cohesion c (kPa)	0.0
Internal friction φ ($^\circ$)	32.5

* σ'_v : Effective overburden pressure (kN/m^2)

4. STUDY OF THREE-DIMENSIONAL DYNAMIC NONLINEAR BEHAVIOR OF PILE FOUNDATION STRUCTURE

Fig. 4.1 shows observed and estimated time histories of accelerations of superstructure, footing and ground surface. In the test, although the horizontal input motion is notably larger in Y direction than in X direction (Fig. 3.5(a), (b)), the horizontal acceleration responses of the soil or the structure do not significantly differ in the two directions (Fig. 4.1(a)-(f)). This indicates the whole test model is showing strong nonlinearity, due to the strong input motion. The analysis can reproduce the horizontal acceleration responses with reasonable degree of accuracy (Fig. 4.1(a)-(f)), although at the ground surface the analysis results are slightly out of phase with observed ones after approximately 5s (Fig. 4.1(c), (f)). Reproducibility by the analysis is clearly lower in the vertical direction than in the horizontal directions, as the estimated and observed results are generally out of phase (Fig. 4.1(g)-(i)). This is probably because the bottom of the analytical model was assumed to be rigid, while in the test, the bottom plate deformed elastically due to the vertical input.

Fig. 4.2 shows bending and axial strains of piles A1, B2 and C3 at pile head (-0.1m) and underground (-1.1m). ∇ and \blacktriangledown marks represent observed and estimated instances when the pile yielded, respectively, determined according to pile axial force (N) – bending moment (M) loci shown in Fig. 4.3. The observed N - M loci are obtained from observed axial and bending strain time histories, assuming that the weight of the structures evenly spread to the each pile and the bending moment was zero at the beginning of the test. Both observed and estimated N - M loci are plotted only until the observed/estimated instance of yielding (Fig. 4.3). The complete list of observed and estimated yielding instances is shown in Table 4.1.

Focusing on pile strain time histories from the test, the bending strains of all three piles show residual

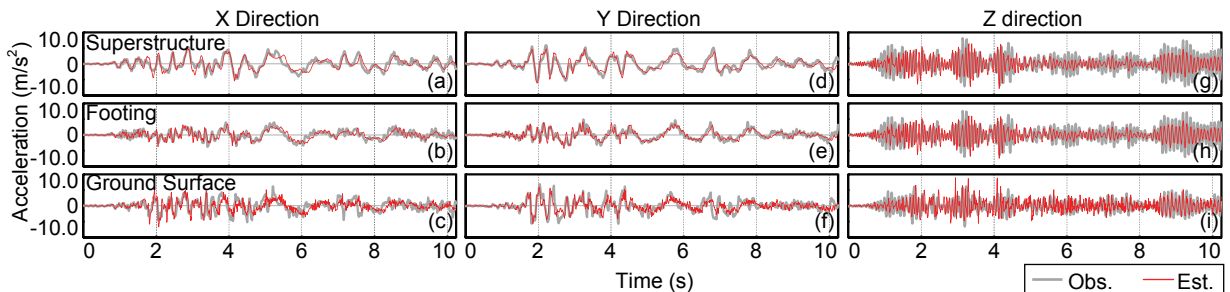


Figure 4.1. Time histories of accelerations

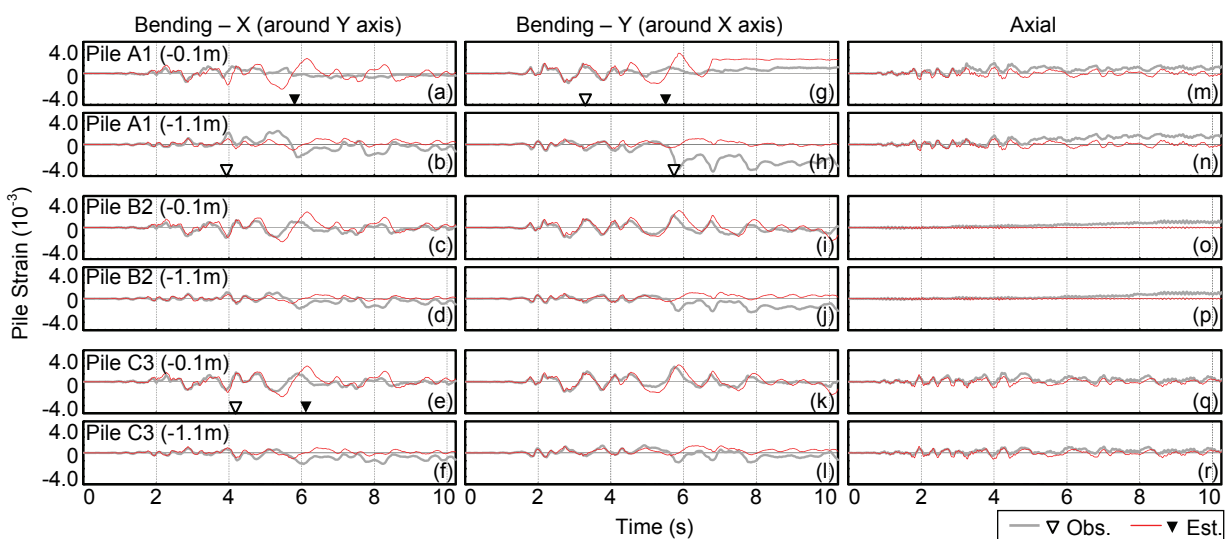


Figure 4.2. Time histories of pile strains

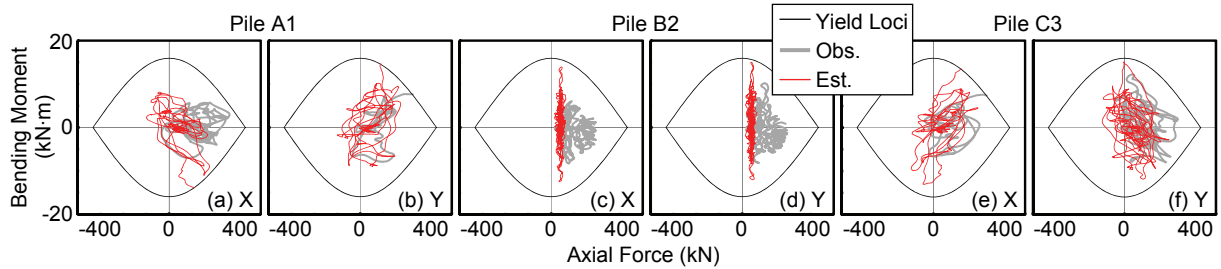


Figure 4.3. Pile axial force – bending moment loci

values, which are more notable underground (Fig. 4.2(a)-(l)). The axial strains of the piles also show residual values on the compression side (Fig. 4.2(m)-(r)). Such values increase as more and more piles yield, becoming significant after 6s, when all piles except B2 and C2 have yielded (Table 4.1). Yielding occurs at almost the same time when the horizontal acceleration of the superstructure takes a peak value (Fig. 4.1(a), (b), Table 4.1), which implies the yielding is likely to be caused by the strong horizontal inertial force coming from the structures.

Notably, the residual values of the axial strain can be seen even before pile A1 first yielded at the pile head at 3.23s (Fig. 4.2(g), (m)), as determined from N-M loci (Fig. 4.3(a), (b), Table 4.1). This implies that pile A1 bore more axial loading than assumed at this instance, which further suggests that the weight of the structures didn't spread evenly to the each pile at the beginning of the test, possibly as a result of the test cases conducted prior to the one discussed in this paper. Due to this fact, the instances when piles yielded in the test, as in Fig. 4.2 \checkmark marks and Table 4.1, may be inaccurate.

While the piles yielded both at pile heads and underground in the test, yielding only occurred at pile heads in the analysis, and the order and the instance of yielding also greatly differ from those in the test (Fig. 4.2, Table 4.1). Despite of this, estimated results are in fairly good agreement with observed ones until about 5s, when corner piles A1, C3 and C1 have yielded in the test but none has yielded in the analysis. This is probably because the possible un-balanced initial state, as discussed in the last paragraph, is not considered in the analysis. As a result, axial forces of the piles are underestimated and too small to reach the yield criteria, although the observed and estimated pile strains are similar. Since the analytical model of the pile does not consider the reduction of axial stiffness after yielding, the estimated results after 5.46s are likely to be unreliable, and will be excluded from further discussions. Estimated and observed bending strains are in relatively better agreement at piles B2 and C3 than at pile A1 (Fig. 4.2(a)-(l)). Axial strains are fairly well reproduced by the analysis, although the estimated results do not show residual values (Fig. 4.2(m)-(r)). Overall, the analysis is able to reproduce the observed tendencies when only a few piles have yielded in the test.

Fig. 4.4 compares observed and estimated vertical distribution of absolute value of maximum shear strain of soil in both horizontal planes, obtained at free field and near piles. The observed and estimated shear strains at free field are calculated from double integral in time scales of acceleration time histories obtained where indicated by ■ marks in Fig. 1. Shear strains near piles are obtained in the same manner, with estimated value using acceleration time histories obtained at the point with distance to center of model of about 1.7 times pile radius, while observed value using those of the center pile itself, since no observation is made in the soil within group pile area and assuming the deformation of the soil and the pile is the same. In the tests, the maximum shear strains in the deeper

Table 4.1. List of instances when piles yielded

Pile	Instance when yielded (Obs. / Est.) [s]			
	X		Y	
	Pile head	Under-ground	Pile head	Under-ground
A1	- / 5.46	3.96 / -	3.23 / 5.80	5.74 / -
A2	- / -	5.75 / -	10.24 / 5.78	- / -
A3	5.86 / 6.06	- / -	7.75 / 5.75	5.7 / -
B1	- / -	5.09 / -	8.5 / -	- / -
B2	- / -	- / -	- / -	- / -
B3	- / 6.12	5.83 / -	- / 5.83	5.8 / -
C1	- / -	5.06 / -	- / 5.85	- / -
C2	- / -	- / -	- / -	- / -
C3	4.21 / 6.13	- / -	- / -	- / -

* “-” denotes no yielding or error in observation data

part of the soil are approximately 1% in average both at free field and near piles (Fig. 4.4(a)-(d)). According to Fig. 3.4, the shear stiffness of the soil has decreased to less than 10% of the initial value, indicating significant progression of nonlinearization of the soil. The maximum shear strains near the surface of the soil are approximately 2-4 times as large as those at free field of the same depth (Fig. 4.4(c), (d)), as a result of soil-pile-structure interaction. The overall tendencies of soil's maximum shear strain distribution are reproduced by the analysis.

Fig. 4.5 shows observed and estimated time histories of absolute value of soil shear strains at the surface of free field (Fig. 4.5(a), (b)) and right beneath the footing near piles (Fig. 4.5(c), (d)), in both horizontal planes. The shear strains are calculated in the same manner as described in Fig. 4.4. At free field, the observed soil shear strain level rises to 1% in both horizontal planes at 2-3s, and decreases afterwards (Fig. 4.5(a), (b)). The estimated value follows the similar trend, but decreases more slowly and becomes larger than the observed one after 6-7s. This probably led to the decrease in reproducibility of horizontal accelerations after about 5s (Fig. 4.1(c), (f)). Near the piles, both observed and estimated soil shear strain are greater than or equal to 1% in both horizontal planes after about 2s (Fig. 4.5(c), (d)), as a result of dynamic interaction between the soil and the piles. Overall tendencies from the test are fairly well-reproduced by the analysis, suggesting the validity of soil's nonlinear model used in the study.

Fig. 4.6-4.9 show observed and estimated bending strain distribution of piles A1, B2 and C3 in Y direction, at four different instances: 2.18s when no pile has yielded in the test (Fig. 4.6), 4.11s when pile A1 has yielded both at the pile head and underground in the test (Fig. 4.7), 5.20s when several more piles have yielded in the test and right before pile A1 yields in the analysis (Fig. 4.8), and at 7.80s when most piles have yielded in both the test and the analysis (Fig. 4.9). At all four instances, the bending strain reaches a peak value at the pile head of center pile B2. In all figures except Fig. 4.8, pile A1 is the leading pile and pile C3 is the trailing pile (Fig. 4.6, 4.7, 4.9); while in Fig. 4.8, pile C3 is the leading pile and pile A1 is the trailing pile (Fig. 4.8).

At 2.18s, all piles are in linear area in both the test and the analysis (Fig. 4.6). Group pile effect can be clearly seen, as the pile bending strain is larger and the depth of inflection point is shallower towards the leading pile. The estimated results are in good agreement with observed ones.

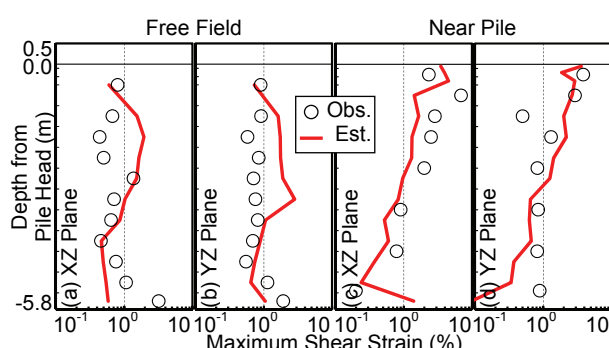


Figure 4.4. Maximum absolute shear strain distribution of soil

At 4.11s, depths of inflection from the test results are deeper in piles B2 and C3 compared to those at 2.18s (Fig. 4.6, 4.7(a), (b)). This is because the soil has softened during the shaking, as seen in the soil shear strain time history presented in Fig. 4.5. However, the inflection point of pile A1 is shallower than that at 2.18s, and the bending strain around the depth of -1.1m is slightly larger (Fig. 4.6, 4.7(c)). This is probably the results of pile A1's yielding at -1.1m at 3.96s (Table 4.1), leading to a residual value in the bending strain at the depth. The analysis is able to reproduce the above

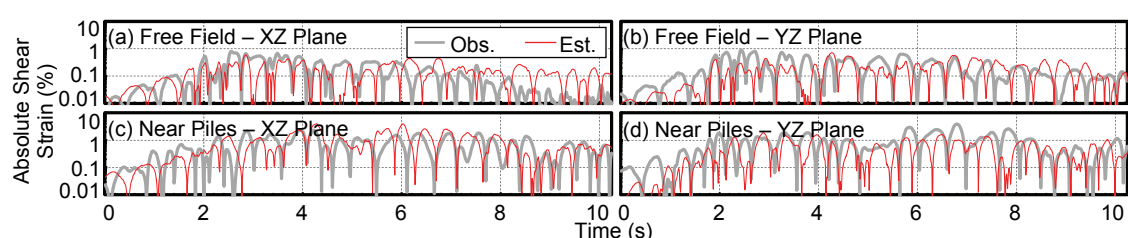


Figure 4.5. Time histories of absolute soil shear strain

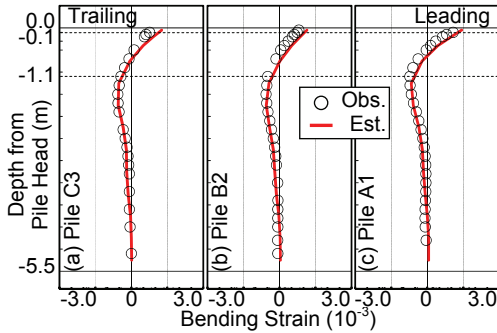


Figure 4.6. Bending strain distributions in Y direction (2.18s)

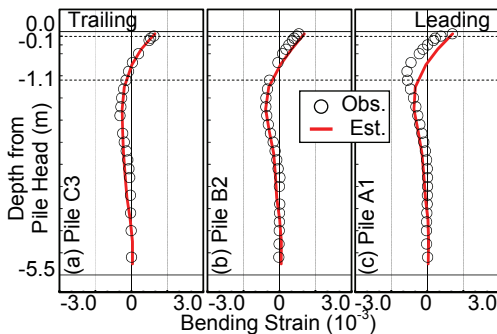


Figure 4.7. Bending strain distributions in Y direction (4.11s)

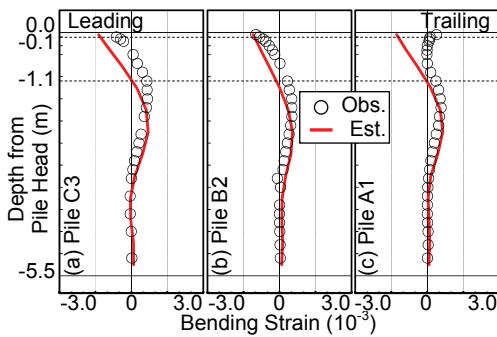


Figure 4.8. Bending strain distributions in Y direction (5.20s)

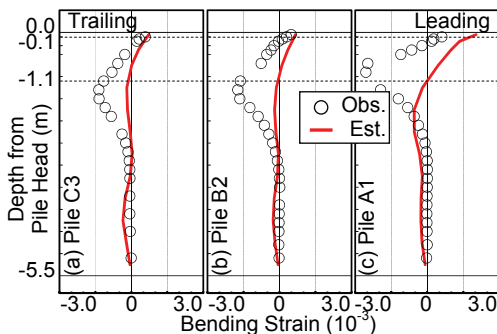


Figure 4.9. Bending strain distributions in Y direction (7.80s)

mentioned tendencies except for pile A1, which hasn't yielded in the analysis.

At 5.20s, in addition to pile A1, pile C3 has yielded at the pile head and piles C1 and B1 have yielded underground in the test (Table 4.1, Fig. 4.8). The bending strain at the pile heads, compared to those at 4.11s, is slightly smaller in pile C3 (Fig. 4.7, 4.8(a)) and significantly smaller in pile A1 (Fig. 4.7, 4.8(c)). This suggests that the bending stiffness at those pile heads has decreased due to the yielding, leading to lower pile head rigidities and smaller bending strains. The analysis, where no pile has yielded yet, overestimates the bending strains at the pile heads of C3 and A1, as well as the depth of inflection points.

At 7.80s, all piles except B2 and C2 have yielded at the pile head and/or underground in the test (Table 4.1, Fig. 4.9). The bending strains around the depth of -1.1m of all three piles are significantly larger than those from the formerly presented instances, as a result of pile damages at the depth. Depths of inflection points are shallow despite of the high soil shear strain level (Fig. 4.5, 4.9), since the pile head rigidities has further decreased due to the yielding at the pile heads. In the analysis, most piles have yielded at the pile heads but all remain in linear zone underground (Table 4.1), and the estimated results greatly differ from the observed ones (Fig. 4.9). This is because the portions where the piles have yielded are different than those in the test, and also due to the limitation of the pile's nonlinear model used in this study.

In general, the analysis is able to reproduce the three-dimensional nonlinear behaviors of the piles with a reasonable degree of accuracy, including the difference between each pile induced by group pile effect, when only a few piles have yielded in the test.

5. CONCLUSIONS

In order to examine the factors influencing the three-dimensional nonlinear behaviors of pile foundation structures during earthquakes, dynamic nonlinear analysis of large shaking table tests where piles yielded are performed using three-dimensional FEM. The following conclusions are obtained.

- (1) In the test, despite the input motion has notably larger horizontal acceleration amplitude in Y direction, the acceleration responses of the superstructure, footing and ground surface do not significantly differ in two horizontal directions. This indicates the whole test model is showing strong nonlinearity, due to the strong input motion. The analysis is able to reproduce the acceleration responses and such tendencies with a reasonable degree of

accuracy.

(2) Piles begin to yield from early stage of the test, because of the large horizontal inertial force from the superstructure, and possibly also due to an un-balanced state of the structures at the beginning of the test. Since the latter factor is not taken into account, piles do no yield in the analysis, despite the piles' bending and axial strains are well-reproduced, at the early stage of the test case.

(3) Piles' observed bending and axial strains show residual values, and such values increase as more and more piles yield. Reproducibility by the analysis declines towards the later stage of the test. The overall result shows, however, that the analysis is able to reproduce the three-dimensional nonlinear behaviors of the piles with a reasonable degree of accuracy, including the difference between each pile induced by group pile effect, when only a few piles have yielded in the test.

ACKNOWLEDGEMENT

The study described herein was made possible through Special Project for Earthquake Disaster Mitigation in Urban Areas, supported by the Ministry of Education, Culture, Sports, Science and Technology (MEXT). The authors express their sincere thanks to the above organization.

REFERENCES

- AIJ (1975). Recommendations for the Plastic Design of Steel Structures, Architectural Institute of Japan (in Japanese).
- Koyamada, K., Miyamoto, Y. and Fukuda, T. (2005). Field Investigation and Analyses Study on Pile Damage of the Tokachi-Oki Earthquake in 2003. *Journal of Structural and Construction Engineering*. No. **589**, 97-104 (in Japanese)
- MEXT and NIED (2006). Research Theme No. 2 Annual Report of the fiscal year 2005. *Special project for earthquake disaster mitigation in urban area*. 489-524 (in Japanese).
- Nakazawa, A., Namba, S., Sotetsu, A., Tokimatsu, K., Oh-oka, H., Shamoto, Y. and Nakazawa, Y. (1999). Investigation on Pile Foundations of High-Rise Buildings Inclined Largely in the Hyogoken-Nambu Earthquake. *Journal of Structural and Construction Engineering*. No. **520**, 69-76 (in Japanese).
- Suzuki, H. and Tokimatsu, K. (2010). Effects of Soil-Structure Interaction on Stress Distribution Within a Pile Group Under Multi-Dimensional Loading. *Proc. of 5th International Conference on Recent Advances in Geotechnical Earthquake Engineering and Soil Dynamics*. Paper No.5.50a.
- Tokimatsu, K., Suzuki, H., Tabata, K. and Sato, M. (2007). Three-dimensional shaking table tests on soil-pile structure models using E-Defense facility. *Proc. of 4th International Conference on Earthquake Geotechnical Engineering*. Paper No. 1529.
- Yoshida, H., Tokimatsu, K., Sugiyama, T. and Shiomi, T. (2008). Practical Three- Dimensional Effective Stress Analysis Considering Cyclic Mobility Behavior. *Proc. of 14th World Conference on Earthquake Engineering*. Paper_ID 04-01-0061.
- Yoshida, H., Ishida, T., Shiomi, T., Hijikata, K., Yanagishita, F., Sugiyama, T., Ohmiya, Y. and Tokimatsu, K. (2006). Study on Practicable 3-Dimensional Effective Stress Analysis Using the Ground Survey Result. *Summaries of technical papers of Annual Meeting AIJ*. **B-1**, 623-626 (in Japanese).
- Yoshida, N., Tsujino, S. and Ishihara, K. (1990). Stress-Strain Model for Nonlinear Analysis of Horizontally Layered Deposit. *Summaries of technical papers of Annual Meeting AIJ*. **B-1**, 1639-1640 (in Japanese).
- Yoshida, N. and Tsujino, S. (1993). A Simplified Practical Stress-Strain Model for the Multi-Dimensional Analysis under Repeated Loading. *Proc. of Annual Conference of the Japan Society of Civil Engineers*. 1221-1224 (in Japanese).
- Zhou, Y., Yoshida, H., Suzuki, H., Nukui, Y. and Tokimatsu, K. (2012). Numerical Study of Three-Dimensional Dynamic Behavior of Soil-Pile-Structure System in Large Shaking Table Tests. *Proc. of 9th International Conference on Urban Earthquake Engineering and 4th Asia Conference on Earthquake Engineering Joint Conference*. 637-643.